Publications of the Astronomical Society of the Pacific, 128:124202 (8pp), 2016 December doi:10.1088/1538-3873/128/970/124202

Orbital Solutions and Absolute Elements of the Massive Algol Binary ET Tauri

Richard M. Williamon[1], Horace Dale[1], Charles L. Evavold[1], Alexander Langoussis[1], Francis C. Fekel[2], Matthew W. Muterspaugh[2,5], Stephen Williams[3,6,7,8], Kate Napier[4], and James R. Sowell[4]
[1] Department of Physics, Emory University, Atlanta, GA 30322, USA; phyrmw1@emory.edu
[2] Center of Excellence in Information Systems, Tennessee State University, Nashville, TN 37209, USA; fekel@evans.tsuniv.edu
[3] Department of Physics and Astronomy, Georgia State University, Atlanta, GA 30303, USA; williams@physics.uoc.gr
[4] School of Physics, Georgia Institute of Technology, Atlanta, GA 30332, USA; jim.sowell@physics.gatech.edu
Received 2016 April 19; accepted 2016 June 25; published 2016 November 1

Abstract

We acquired differential *UBV* photoelectric photometry and radial velocities of the relatively bright, understudied, massive Algol binary ET Tau and utilized the Wilson-Devinney (WD) analysis program to obtain a simultaneous solution of these observations. To improve the orbital ephemeris, the *V* measurements from the *ASAS* program were also analyzed. Because of the very rapid rotation of the significantly more massive and hotter component (B2/3 spectral class), only radial velocities of the secondary component, which has a ~B7 spectral class, could be measured. We derive masses of $M_1 = 14.34 \pm 0.28\,M_\odot$ and $M_2 = 6.339 \pm 0.117\,M_\odot$ and equal-volume radii of $R_1 = 6.356 \pm 0.056\,R_\odot$ and $R_2 = 11.84 \pm 0.10\,R_\odot$ for the primary and secondary, respectively. The secondary is filling its Roche lobe, so the system is semi-detached. The effective temperature of the secondary was held fixed at 15,000 K, and the primary's temperature was found to be 30,280 ± 109 K. The system, which has a period of 5.996883 ± 0.000002 days, is assumed to have a circular orbit and is seen at an inclination of 79°.55 ± 0°.05.

Key words: binaries (including multiple): close – binaries: eclipsing – binaries: spectroscopic – stars: individual

Online material: color figures, machine readable tables

1. Introduction

ET Tau = HD 245523 is a relatively bright ($V = 8.79$ mag), high-mass Algol binary, for which there is only a modest amount of information in the literature. From photographic plates, Shakhovskoy (1955) obtained a period of 5.996879 days, an ephemeris, and a light curve for this partially eclipsing binary. Wood & Forbes (1963) re-analyzed the Shakhovskoy data and produced an improved epoch and period (5.996918 days). Three Strömgren observations were acquired by Hilditch & Hill (1975), and their two ($b - y$) values outside of eclipse averaged to +0.315 ± 0.005 mag, suggesting that if there is no reddening, the primary component is an F star (Allen 2000). Brancewicz & Dworak (1980) included ET Tau as one of more than 1000 eclipsing binaries for which parameters were determined from literature data. They used an "iterative" method to compute geometric and physical parameters. Their results described a semi-detached system with a B8 primary and an early F secondary. In his catalog, Budding (1984) noted that there could be solution errors for ET Tau. Later, Budding et al. (2004) gave basically the same parameter values as before, but did include $B - V = 0.262$ mag, a value that corresponds to a late A star (Allen 2000). Polidan & Wade (1991) acquired low-dispersion *IUE* spectra of ET Tau, but a full analysis of those spectra was never published. The system was not observed by *Hipparcos*.

We present complete *UBV* differential light curves along with partial light curves from two other sources. In addition, we obtained a high-resolution blue-wavelength spectrum showing features of both components and more than 100 echelle spectra from which we measured radial velocities of a single component. The RV and photometric data sets were solved simultaneously with the Wilson-Devinney (WD) program, and the orbital elements and absolute dimensions of both the system and of each component have been determined. The solution has the secondary filling its Roche lobe. Our analyses show that the ET Tau system differs greatly from previous solutions found in the literature.

[5] College of Life and Physical Sciences, Tennessee State University, Nashville, TN, USA matthew1@coe.tsuniv.edu
[6] Now at: Foundation of Research and Technology-Hellas, 71110, Heraklion, Crete, Greece.
[7] Now at: University of Crete, Physics Department & Institute of Theoretical & Computational Physics, 71003, Heraklion, Crete, Greece.
[8] Visiting Astronomer, National Optical Astronomy Observatories (NOAO). NOAO is operated by the Association of Universities for Research in Astronomy (AURA), under contract with the National Science Foundation.

Table 1
Fernbank Photometric Observations of ET Tau

Helio. Julian Date (HJD − 2400000)	ΔV (mag)	Helio. Julian Date (HJD − 2400000)	ΔB (mag)	Helio. Julian Date (HJD − 2400000)	ΔU (mag)
45339.5920	−0.5567	45339.5927	−0.4105	45339.5934	−0.6124
45339.5955	−0.5544	45339.5959	−0.3973	45339.5965	−0.5991
45339.6030	−0.5471	45339.6036	−0.3981	45339.6044	−0.6011
45339.6065	−0.5548	45339.6070	−0.3962	45339.6080	−0.5998
45339.6164	−0.5433	45339.6172	−0.3895	45339.6177	−0.5836

(This table is available in its entirety in machine-readable form in the online version of this article.)

2. Photometric Observations and Reductions

The main set of our photometric observations was obtained in 1984–1986 with the 36-inch reflector at the Fernbank Science Center (Atlanta, GA). Standard *UBV* filters were used with an unrefrigerated EMI 6256S photomultiplier to closely approximate the effective wavelengths of the Johnson-Morgan system. The observations were recorded with a Honeywell strip-chart recorder, and deflections were read with a 5 s timing accuracy. All measurements of ET Tau were made differentially with respect to the comparison star HD 37800, and HD 37424 was used as the check star. The observations were corrected for atmospheric extinction by means of nightly coefficients determined from the comparison star via the technique of Hardie (1962). The heliocentric Julian dates and differential magnitudes for the 655 V, 650 B, and 631 U data are provided in Table 1.

A second set of V photometry, obtained during 2003, is from the *All Sky Automated Survey* (*ASAS*)-3 project of Pojmanski (2002). This automated observational program obtained one or two V measurements per night. With each observation, a quality code of A through D was assigned, and we only used the highest-quality A values. After visually removing a few points that had large deviations from the data, the final set contained 154 observations and these are given in Table 2. The *ASAS* data were used to improve the epoch and period since those observations were acquired more than 15 years after ours.

A few observations of ET Tau were taken through Johnson *BVR* filters at the Emory University Observatory in 2013. We used a 12.7-cm Meade telescope with an SBIG ST-10XME CCD camera cooled to −20° C. The measurements were reduced with Maxim DL software. The comparison and check stars were HD 37241 and GSC 1869-686, respectively. We used the data collected on HJD 2456340 because the corresponding ∼0.72 phase was a rare time where the light curves are flat. The approximately 70 individual measurements per bandpass are listed in Table 3. These data established the *BVR* relationships and refined the surface temperature of the primary.

Table 2
ASAS Photometric Observations of ET Tau

Helio. Julian Date (HJD − 2400000)	V (mag)	Helio. Julian Date (HJD − 2400000)	V (mag)	Helio. Julian Date (HJD − 2400000)	V (mag)
52621.7035	8.806	52702.5431	8.976	52978.7388	8.804
52621.7354	8.813	52702.5556	8.927	52984.7070	8.827
52623.6740	8.856	52704.5317	8.780	52985.7260	8.707
52623.6923	8.843	52706.5328	8.717	52986.7235	8.845
52625.6960	8.688	52711.5115	8.879	52987.7454	8.779

(This table is available in its entirety in machine-readable form in the online version of this article.)

Table 3
Emory Photometric Observations of ET Tau

Helio. Julian Date (HJD − 2400000)	V (mag)	Helio. Julian Date (HJD − 2400000)	B (mag)	Helio. Julian Date (HJD − 2400000)	R (mag)
56340.572	8.732	56340.571	9.182	56340.573	8.447
56340.575	8.745	56340.574	9.175	56340.575	8.450
56340.577	8.736	56340.576	9.180	56340.578	8.452
56340.579	8.737	56340.579	9.177	56340.580	8.449
56340.582	8.738	56340.581	9.175	56340.582	8.446

(This table is available in its entirety in machine-readable form in the online version of this article.)

3. Spectroscopic Observations and Reductions

In 2008 and 2009, we obtained several high-resolution spectral observations with the Kitt Peak National Observatory 0.9-m coudé feed telescope. We used the long collimator and grating A (632 grooves per mm with blaze wavelength 6000 Å) in second order with the 4–96 order sorting filter. The F3KB detector has a 3072 × 1024 pixel array with 15 × 15 square μm pixels,

and this instrument provided a resolving power of $R = \lambda/\Delta\lambda = 14900$ in the wavelength range from 4310 to 4635 Å. The observations were not flux calibrated.

From 2012 April to 2015 February we acquired 106 spectra of ET Tau with the Tennessee State University (TSU) 2-m automatic spectroscopic telescope (AST) and a fiber-fed echelle spectrograph (Eaton & Williamson 2007), which is situated at Fairborn Observatory in southeastern Arizona. The detector was a Fairchild 486 CCD, having 4000 × 4000 15 μm pixels. At 6000 Å, the echelle spectrograms have a resolving power of 15,000 and a typical signal-to-noise ratio (S/N) of 90 to 160. Because of the significantly reduced efficiency of the spectrograph at blue wavelengths, we have used just the 4920–7100 Å region.

Fekel et al. (2009) provide a general description of velocity measurements from the Fairborn Observatory echelle spectra. Given the B spectral types of ET Tau, there are very few prominent lines. The Hα profile is asymmetric, and that asymmetry shifts from side to side indicating that both binary components contribute to the spectrum. Several different line lists were used before finally settling on one that included just the He I lines at 5875.6 Å and 6678.1 Å. With that list only one stellar component could be detected, and its lines were significantly variable in strength. Rotationally broadened profiles (Fekel & Griffin 2011) were fit to the observed features. Based on the 20 spectra with the best S/N and relatively symmetric, strong line profiles, the $v \sin i$ value of the secondary is 78 ± 3 km s^{-1}.

The Fairborn AST velocities are on an absolute scale. Unpublished measurements of several IAU solar-type velocity standards show that the Fairborn Observatory velocities with the Fairchild CCD have a zero-point offset of −0.6 km s^{-1} relative to those of Scarfe (2010). Thus, +0.6 km s^{-1} has been added to each of our velocities. Table 4 provides the heliocentric Julian dates of mid-observation and the velocities of the single component.

Table 4
Radial Velocity Observations of ET Tau

Helio. Julian Date (HJD − 2400000)	Phase	RV (km s^{-1})	$O - C$[a] (km s^{-1})
56028.636	0.439	−196.4	−1.7
56029.636	0.606	−171.9	−3.7
56196.820	0.484	−219.9	−9.6
56215.877	0.662	−95.1	+17.4
56232.840	0.491	−213.0	−1.8
56252.019	0.689	−86.5	−6.1
56267.891	0.336	−101.5	+1.7
56290.842	0.163	+129.1	+9.4
56308.909	0.176	+118.6	+13.8
56329.836	0.665	−100.8	+8.2
56339.617	0.296	−54.0	+0.0
56340.617	0.463	−226.3	−21.3
56341.663	0.637	−133.9	+5.3
56346.614	0.463	−214.0	−9.0
56347.614	0.630	−144.1	+2.7
56348.615	0.797	+64.4	+1.8
56348.738	0.817	+87.3	−1.5
56349.681	0.975	+236.3	+19.9
56350.619	0.131	+153.8	+0.0
56351.621	0.298	−59.2	−3.0

Note.
[a] $O - C$ = observed radial velocity minus that determined from the orbital elements for the velocity curve.

(This table is available in its entirety in machine-readable form in the online version of this article.)

Table 5
Spectroscopic Orbital Elements of the ET Tau Secondary[a]

Parameter	Value
P (days)	5.996883[b]
T_0 (HJD)	2, 456, 553.7458 ± 0.0056
e	0.0[b]
ω (deg)	0.0[b]
K (km s^{-1})	215.8 ± 1.3
γ (km s^{-1})	4.02 ± 0.90
RV rms (km s^{-1})	9.1
f(m) ($M_\odot$)	6.24 ± 0.11
$a \sin i$ (10^6 km)	17.79 ± 0.10

Notes.
[a] Solution computed from the Fairborn Observatory data alone.
[b] Adopted value.

4. Spectroscopic Orbit

We adopted an eclipse period of 5.996883 days and computed an orbital solution of the single component with SB1C (D. Barlow, 1998, private communication), a computer program that produces a circular orbit solution. For such an orbit, the element T, time of periastron passage, is undefined, and, as recommended by Batten et al. (1989), T_0, a time of maximum velocity is given instead. Table 4 includes the fractional phases referenced to that epoch and the velocity residuals determined from the circular orbit fit. The time of maximum velocity for this component occurs 0.25 orbital phase units after primary eclipse.

The spectroscopic orbital solution (Table 5) gives a center-of-mass velocity of 4.0 ± 0.9 km s^{-1} and a semi-amplitude of 215.8 ± 1.3 km s^{-1}. Of particular interest is the mass function computed from the orbital elements. Its value of 6.2 ± 0.1 $M_\odot$ is extremely large, and this result is discussed in the next section.

5. Combined Light and Velocity Solution

There was little information from the literature to incorporate at the beginning of our analysis. Prior to the acquisition of our

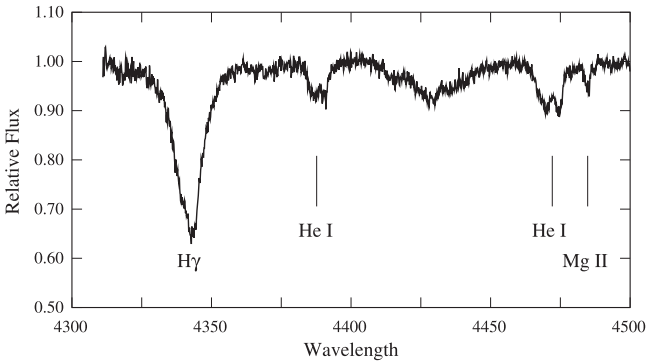

Figure 1. High-resolution spectrum of ET Tau, obtained with the KPNO coudé feed telescope, shows a very blended Hγ line. The He I 4387 Å and He I 4471 Å lines are partially resolved into two components with the broader-lined component being blueshifted. The Mg II line at 4481 Å is only that of the cooler star. This plot is a combined spectrum of two 1800 s exposures with a mean observation time of HJD 2454802.7887 (UT date 2008 December 2).

own spectroscopy we corresponded with G. Peters (2002, private communication), who had spectra of ET Tau. She reported to us that two sets of spectral lines were visible for this system, a relatively sharp redshifted feature and a quite broad blueshifted component. Her estimated spectral classes were B2 or possibly B3 for the broad-lined component and B7 for the narrow-lined one.

In the wavelength region of the echelle spectra where we measured our velocities, the very broad Hα line appears to be a blend of both components and no other lines from the broad-lined star are obvious. Our blue-wavelength coudé feed spectrum (Figure 1) shows that Hγ is asymmetric in shape, and thus the two components are extensively blended. The He I 4387 Å and He I 4471 Å lines of both components are present and partially resolved with the broad-lined star being blueshifted, while the weak Mg II 4481 Å line appears in just the narrower-lined star. From the He I lines of the more rapidly rotating blueshifted component, we estimate a $v \sin i$ value of 250–300 km s^{-1}. The lack of a Mg II line for that component indicates that it is the hotter star. These results are in accord with the estimated spectral classes of Peters.

The above discussion indicates that the lines measured for radial velocity in our echelle spectra are from the cooler, slower rotating star. However, the huge value of the mass function, 6.2 $M_\odot$ (Table 5), indicates that the measured component is the less massive rather than the more massive star. For example, if we adopt a mass of 5 $M_\odot$ for the mass of the (late B) star whose spectroscopic orbit we have determined and assume 80° for the orbital inclination, then from the mass function the mass of the unmeasured component is 12.5 $M_\odot$.

In contrast to the spectral classifications are the existing photometric color indices. The $B - V$ value of +0.262 mag from Budding et al. (2004) and the average $(b - y)$ of

Table 6
WD Measurement Characteristics of the ET Tau Observations

Curve	Observatory	Data Points	Normal Mag[a]	σ
V	Fernbank	655	−0.538	0.012
B	Fernbank	650	−0.382	0.012
U	Fernbank	631	−0.585	0.019
V	*ASAS*	154	+8.718	0.018
V	Emory	68	+8.752	0.005
B	Emory	71	+9.185	0.004
R	Emory	67	+8.445	0.006
RV_2	TSU	106	⋯	10 km s^{-1}

Note.
[a] The normalization magnitude used in the WD program.

Table 7
Non-varying WD Parameters

Parameter	Symbol	Value
Albedo (bol)	A_1, A_2	1.00, 1.00
Gravity Darkening	g_1, g_2	1.00, 1.00
Limb Darkening (bol)	x_1, y_1	+0.252, +0.512
Limb Darkening (bol)	x_2, y_2	+0.612, +0.123
Limb Darkening (*R*)	x_1, y_1	−0.134, +0.563
Limb Darkening (*R*)	x_2, y_2	−0.079, +0.579
Limb Darkening (*V*)	x_1, y_1	−0.134, +0.627
Limb Darkening (*V*)	x_2, y_2	−0.065, +0.654
Limb Darkening (*B*)	x_1, y_1	−0.137, +0.689
Limb Darkening (*B*)	x_2, y_2	−0.041, +0.717
Limb Darkening (*U*)	x_1, y_1	−0.100, +0.647
Limb Darkening (*U*)	x_2, y_2	+0.025, +0.599

0.315 mag from Hilditch & Hill (1975) must both be highly reddened since the color index for a B7 star is negative (Flower 1996). The average $(u - b)$ and $(v - b)$ indices of 0.729 and 0.275 mag from Hilditch & Hill (1975) give the c_1 parameter as 0.454 mag, and it falls in the mid-B range (Allen 2000).

The combined light and velocity curve solutions were computed with the 2013 version of the WD program. The physical model of that program is described in detail in Wilson & Devinney (1971), Wilson (1979, 1990, 2012a, 2012b), Van Hamme & Wilson (2007), and Wilson et al. (2010). All observations in each data set were assigned a weight of 1. Our curve-dependent weights were computed from the standard deviations listed in Table 6. Light level-dependent weights were applied inversely proportional to the square root of the light level. Gravity darkening (g) and bolometric albedo (A) coefficients were fixed at the radiative-envelope, canonical values of 1.00 from Lucy (1967) for both stars. We adopted a square-root limb-darkening law with coefficients x, y from Van Hamme (1993) for both components, and the detailed reflection

treatment of Wilson (1990) was used with two reflections. Table 7 contains the values of our non-varying parameters.

We used the orbital elements from our preliminary spectroscopic solution as criteria to be met by our ultimate combined solution, in particular for restricting the semimajor axis and the resulting value of the semi-amplitude of the secondary. The shapes of the *UBV* light curves indicated at least one Roche lobe should be filled, so we used Mode 5 to set the secondary's size at this limit. Adopting a B7 classification for the secondary, we initially fixed its temperature at 12,500 K, from the tables of Allen (2000). We performed WD runs that varied the mass ratio, size and temperature of the primary, the inclination, semimajor axis, radial velocity of the center of mass, the epoch, period, and light normalization parameters. After the solution was found, we adjusted the secondary's temperature in steps of 500 K and re-determined the solution using all of the variable parameters. The smallest sum of the squares of the residuals corresponded to a temperature of 15,000 K.

In addition, the rotation parameters (F) for the primary and secondary were carefully considered. These factors give the rotation speeds relative to the orbital velocities. The estimated rotation speed from fitting a profile to the high-resolution spectrum was 250–300 km s^{-1} for the primary. Using a velocity of 275 km s^{-1} and initial solutions that provided the radii of both stars in solar units and the orbital period in days, the F values were computed. Then, new solutions were found, and it only took a couple of iterations to obtain resulting radii that were equal to the initial values. The primary's F value was set at 5.2. For the secondary, from the fitted profile, we derived $F = 0.8$; however, given the assumption that its Roche lobe is filled, the rotation is expected to be synchronous ($F = 1.0$). We obtained WD solutions using both of these values. (Note that Mode 5 does not require that the secondary has synchronous rotation.) We anticipated that there would be little difference in the solution values and errors, but this was not the case for every parameter. We report in the text and tables the values from the synchronous rotation solution, but we have increased the listed errors for the parameters that deviated. With our spectral fitting indicating non-synchronous rotation, we ran Mode 2 simulations to check to see if the Roche-lobe filling is not valid, but these solutions gave the secondary's size slightly larger than that of the lobe. See Van Hamme & Wilson (1993) for a description of a similar scenario regarding the F parameters in the solutions of two Algols.

We also attempted to solve the ET Tau data with the Mode 6 option of the WD program, which is for double contact binaries where both limiting lobes are filled but the stars are not necessarily touching. Mode 6 expects that one of the components has a non-synchronous rotation. (Refer to Wilson & Van Hamme 1986 for further information on this mode.) All of the same parameters for the Mode 5 solution were again allowed to vary, except for the size of the primary since this mode applies surface potential constraints on both stars. No solution convergence was found with a range of F parameter values near those based on the spectroscopic rotation rates. We allowed the F terms to vary, and a solution was obtained. However, the resulting $F_1 = 7.85$ value corresponds to a rotation speed of 450 km s^{-1}, which is significantly higher than the 275 km s^{-1} we have utilized from the line profile analysis. Given our incomplete photometric coverage of the secondary eclipse, we place a higher confidence on the spectroscopic broadening estimate than on the WD value for F_1; consequently, we prefer the Mode 5 solution and scenario.

Table 8
Light and Velocity Curve Results for ET Tau[a]

Parameter	Symbol	Value
Inclination (deg)	i	79.55 ± 0.05
Semimajor axis ($R_\odot$)	a	38.13 ± 0.26
Mass ratio	M_2/M_1	0.442 ± 0.010
Surface potential	Ω_1	6.822 ± 0.041
Surface potential	Ω_2	2.763[b]
Temperature (K)	T_1	30, 280 ± 109
Temperature (K)	T_2	15, 000[c]
Rotation Factor	F_1	5.2[c]
Rotation Factor	F_2	1.0[c]
Eccentricity	e	0.0[c]
Systemic velocity (km s^{-1})	γ	+3.79 ± 0.89
Primary's speed (km s^{-1})	K_1	96.94 ± 1.00[d]
Secondary's speed (km s^{-1})	K_2	219.3 ± 2.2[d]
Period (days)	P	5.9968833 ± 0.0000019
Epoch (HJD)	T_0	2, 446, 033.6954 ± 0.0004
Luminosity ratio (R)	$L_1/(L_1 + L_2)$	0.4800 ± 0.0053
Luminosity ratio (V)	$L_1/(L_1 + L_2)$	0.5005 ± 0.0044
Luminosity ratio (B)	$L_1/(L_1 + L_2)$	0.5270 ± 0.0045
Luminosity ratio (U)	$L_1/(L_1 + L_2)$	0.6205 ± 0.0057

Notes.
[a] Wilson-Devinney simultaneous solution, including proximity and eclipse effects, of the light and velocity data.
[b] Set equal to the surface potential of the component's limiting lobe.
[c] Adopted value, see Section 5 in the text.
[d] The error is assumed to be about 1%.

The orbital elements and absolute dimensions for the solution of a semi-detached system with the secondary in synchronous rotation are given in Tables 8 and 9, respectively. We note that in Table 8 the effective temperature of the secondary has no uncertainty, and the uncertainty given for the primary's effective temperature is the uncertainty of the temperature difference. To estimate an uncertainty for the secondary's temperature, as noted earlier, we obtained WD solutions with the temperature of the secondary changed in steps of 500 K. This resulted in temperature uncertainty estimates of about ±300 K for both components.

From Table 9 the absolute dimensions include masses of $M_1 = 14.34 \pm 0.28\,M_\odot$ and $M_2 = 6.34 \pm 0.12\,M_\odot$ and

Table 9
Fundamental Parameters of ET Tau

Parameter	Primary	Secondary
M ($M_\odot$)	14.34 ± 0.28	6.34 ± 0.12
R ($R_\odot$)	6.356 ± 0.065	11.84 ± 0.10
$L/L_\odot$	30450 ± 1344	6367 ± 356
M_{bol} (mag)	−6.459 ± 0.048	−4.760 ± 0.061
log g (cm s^{-2})	3.99 ± 0.01	3.09 ± 0.01
T (K)	30,280 ± 109	15,000[a]

Note.
[a] Adopted value, see Section 5 in the text.

equal-volume radii of $R_1 = 6.356 \pm 0.065\,R_\odot$ and $R_2 = 11.84 \pm 0.10\,R_\odot$. Figure 2 plots our *UBV* measurements with the light curves computed for each bandpass. The residuals to the fits are graphed in Figure 3. The *ASAS* and RV data are shown in Figures 4 and 5, respectively, with the corresponding WD best-fit curves overplotted.

The WD solution, with the radial velocity lines assigned to the secondary, has several details to be highlighted. (1) Our secondary semi-amplitude of 219.3 ± 2.2 km s^{-1} is very close to the 215.8 ± 1.3 km s^{-1} value found from the initial spectroscopic orbit solution. (2) Due to the scenario of a rapidly rotating primary star, the rotation parameter F_1 was set at 5.2 times that of the synchronous speed. (3) A mass ratio of 0.442 ± 0.004 was determined. (4) An improved ephemeris for the midpoint of primary eclipse is

$$\mathrm{HJD(min)} = 2{,}446{,}033.6954 \pm 0.0004 + 5.9968833 \pm 0.0000019 \times E.$$

(5) The mass for our ~B7 star (6.34 ± 0.12 $M_\odot$) is slightly larger than the B5 5.9 $M_\odot$ value given by Allen (2000). We recognize that (a) there is some uncertainty in both the spectral classification of ET Tau and in the canonical masses for B stars and that (b) the secondary is not on the main sequence and mass exchange has probably occurred in the past.

The WD program computes geometrical sizes of the two stars. Relative radii are given in four directions: from the center toward the poles, toward the sides, toward the back, and toward the point. The WD program computes an "equal-volume," mean radius ($\langle r \rangle$) and the percentage of the Roche lobe ($\langle r \rangle / \langle r \rangle_{lobe}$) that is filled, being 72% and 100% for the primary and secondary. The relative radii are listed in Table 10, and Figure 6 is an image of the system at phase 0.25 to demonstrate the relative shapes.

6. Comparison of Results

Brancewicz & Dworak (1980) used an "iterative" method to derive geometric and physical parameters of the components for more than 1000 binaries. Using basic astronomical equations, e.g., Kepler's third law, and observed (or assumed)

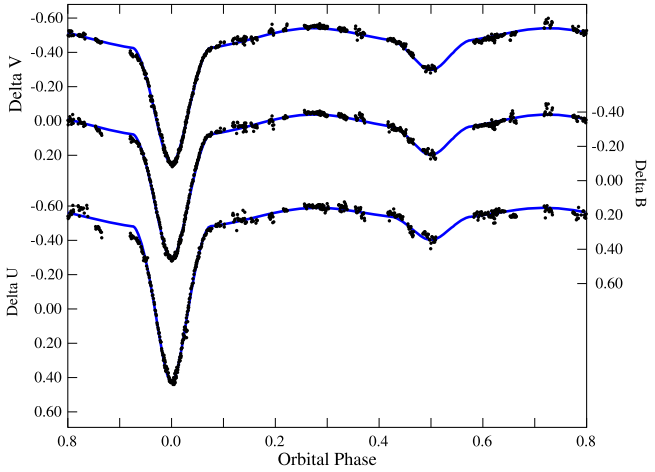

Figure 2. Our differential *UBV* magnitudes of ET Tau are plotted with the Wilson-Devinney solution curves based on the photometric sets and the RV measurements. The system is a hot Algol type, with the secondary filling its Roche lobe.
(A color version of this figure is available in the online journal.)

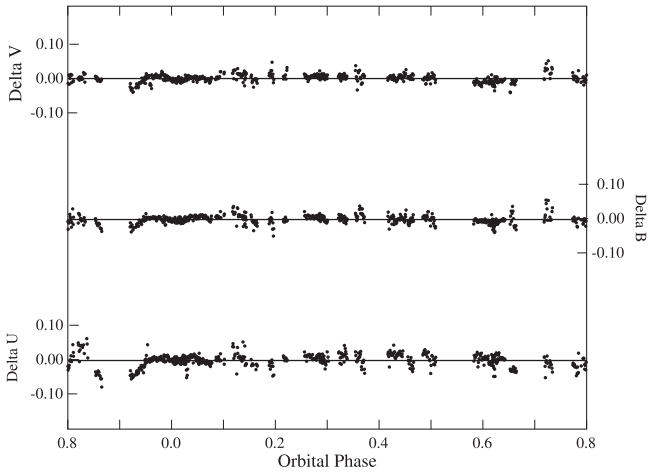

Figure 3. Residuals to the fit of our *UBV* photometry using the solution light curves. The vertical scale is twice that of Figure 2.

quantities such as the orbital period, spectral types, mass ratio, and relative radii, they computed the parallax, separation between the components, radii in solar units, percentage of Roche-lobe filling, luminosities, temperatures, sum of the masses, mass ratio, and mass of the primary. For ET Tau, they assumed the primary had the spectral classification of B8, and they derived a mass of 4.70 $M_\odot$, temperature of 10,680 K, and radius of 5.04 $R_\odot$. The secondary, though, had a 6,720 K temperature and radius of 9.96 $R_\odot$, which was overfilling its Roche lobe at 121%. With their mass ratio of 0.45, the secondary's mass was 2.1 $M_\odot$. Other quantities included a distance of 1,100 pc and a separation of 26.36 $R_\odot$. Without the

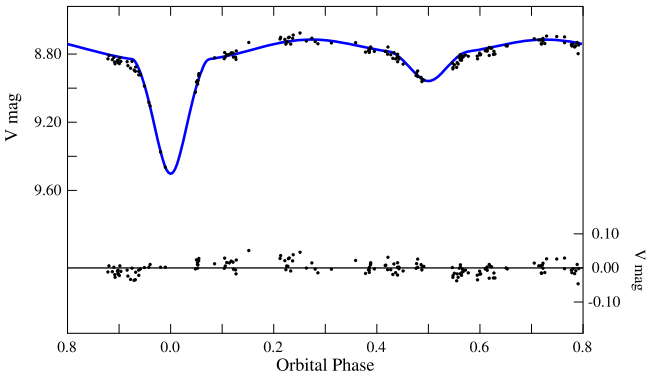

Figure 4. *ASAS* differential *V* magnitudes (Pojmanski 2002) of ET Tau are plotted with the Wilson-Devinney solution curves based on the three photometric data sets and the RV measurements. Residuals to the fit, provided by the solution light curve, are plotted at the bottom of the figure. The vertical scale for the residuals is twice that of the light curve.
(A color version of this figure is available in the online journal.)

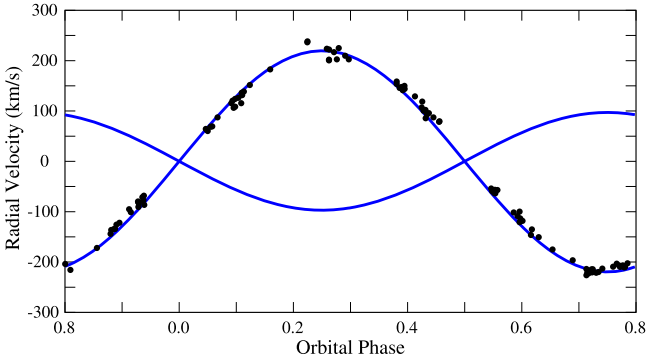

Figure 5. Our radial velocities of ET Tau are plotted with the Wilson-Devinney solution curves for the combined photometric and RV data. Zero phase is at the time of primary eclipse.
(A color version of this figure is available in the online journal.)

Table 10
Model Radii for ET Tau

Parameter	Value
r_1 (pole)	0.1566 ± 0.0008
r_1 (point)	0.1731 ± 0.0012
r_1 (side)	0.1722 ± 0.0012
r_1 (back)	0.1729 ± 0.0012
$\langle r_1 \rangle$[a]	0.1667 ± 0.0010
$\langle r_1 \rangle / \langle r_1 \rangle_{\rm lobe}$	0.7157 ± 0.0060
r_2 (pole)	0.2905 ± 0.0007
r_2 (point)	0.4174 ± 0.0007
r_2 (side)	0.3030 ± 0.0008
r_2 (back)	0.3356 ± 0.0008
$\langle r_2 \rangle$[a]	0.3106 ± 0.0015
$\langle r_2 \rangle / \langle r_2 \rangle_{\rm lobe}$	1.0000 ± 0.0000

Note.
[a] "Equal volume" mean radii.

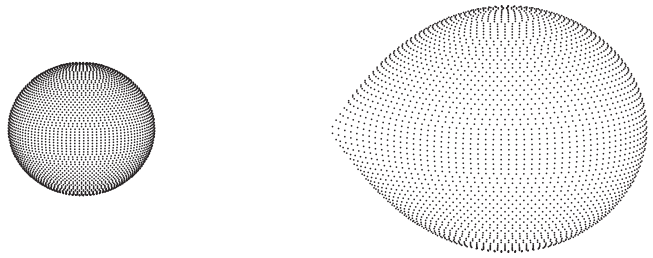

Figure 6. Gravitational distortion of the ET Tau components' shapes are shown at phase 0.25. The smaller, hotter, more massive primary is rotating 5.2 times faster than the synchronous rate. The secondary is filling its Roche lobe and is rotating synchronously. The relative radii are given in Table 10.

spectroscopic observations that led to our greatly improved spectral types and velocities of the secondary, these results seemed reasonable, but now this solution can be rejected.

The Approximate Elements of Eclipsing Binaries by Svechnikov & Kuznetsova (1990) assumed the spectral types were B8 and A5. The masses were 4.00 $M_\odot$ and 2.40 $M_\odot$, and the radii corresponded to 5.00 $R_\odot$ and 8.45 $R_\odot$. The semimajor axis was 25.80 $R_\odot$, and the inclination of 80°.5 was close to our value. Again, without our B spectral types and the secondary's radial velocities, this study gives typical results for Algol binaries, including the secondary having the larger radius, but it too can now be excluded.

7. Discussion

Hilditch & Bell (1987) compiled a list of 31 binary systems with a spectral type of B5 or earlier. Their list included eight with semi-detached configurations, and recent investigations of four of them, u Her, TT Aur, AI Cru, and Z Vul, have some relevancy to ET Tau. See Nelson & Eggleton (2001) regarding their evolution. We also discuss a fifth binary, MR Cyg.

The system u Her = HR 6431 (Hilditch 2005) consists of B2 and B8 stars and has had a constant orbital period for almost a century. Hilditch notes that the scatter in all photometric measurement sets is larger than expected, and he considers that the intrinsic variability may be due either to gas streams or perhaps β Cephei-like pulsations. Outside of the ET Tau eclipses, our photometry has some scatter, and in particular, prior to the primary's first contact is a depression seen in all three *UBV* light curves, which might be due to similar processes.

MR Cyg has been the subject of study by many groups, and a wide range of mass ratios have been obtained. The analysis by Linnell et al. (1998) gives the primary's mass as 8.00 ± 0.30 $M_\odot$ and the secondary's as 3.19 ± 0.08 $M_\odot$. Their photometric data deviate from the theoretical curves in two

phase ranges; they argue it could be due to seeing effects, but we raise the possibility that this might be another example of intrinsic variability. They posit that MR Cyg has just entered a phase of slow mass transfer, but they reiterate the suggestion by Chiosi & Maeder (1986) that the primary may be losing mass via a wind. The orbital period has been constant.

Özdemir et al. (2001) determined the TT Aur component masses as $7.2 \pm 0.1\ M_{\odot}$ and $4.80 \pm 0.03\ M_{\odot}$. They noted that their light curves (see their Figure 4) "tend to show absorption effects in the primary minimum, which may also relate to mass transfer." This is similar to the depression seen in our light curves just before primary eclipse at about phase 0.9 (see Figure 2). In discussing the *U*-band primary eclipse, they suggest there is a hotter region on the secondary, due to the impact of mass transfer. TT Aur shows a long-term period change, which could possibly be due to mass loss.

AI Cru has masses of $10.3 \pm 0.2\ M_{\odot}$ and $6.3 \pm 0.1\ M_{\odot}$ according to Bell et al. (1987). Zhao et al. (2010) believe AI Cru is now in a slow phase of mass transfer and that this rate is too low to cause the observed rate of period increase. They, too, suggest that mass loss from the detached primary via a stellar wind is the cause for the period increase.

Finally, in the orbital solution of Z Vul by Lazaro et al. (2009), they determined masses of $5.3 \pm 0.5\ M_{\odot}$ and $2.3 \pm 0.2\ M_{\odot}$ for the primary and secondary, respectively, and found that adopting the primary's rotation rate to be faster than synchronous produced better fits to the light curves. They commented that adjusting the rotation speed is preferred over changing the gravity-darkening parameter of the secondary. As previously described for ET Tau, we allowed the rotation parameter to vary and used the canonical value of 1.00 from Lucy (1967) for both radiative envelopes.

Although the components of ET Tau are somewhat hotter and more massive (see Tables 8 and 9) than the components of the above systems, our review of those five somewhat similar hot Algols indicates that future observational programs on ET Tau should (a) investigate the possibility of intrinsic photometric variability, (b) search for mass loss by stellar winds, and (c) begin long-term monitoring for orbital period changes. When computing solutions on such systems, one should always allow for non-synchronous rotation.

We thank Walter Van Hamme (Florida International University) for valuable discussions about this system and about the WD program's various modes. In addition, he graciously computed the error bars of the parameters in the final solution. We note that the anonymous referee's comments guided us in making a substantially improved paper. We appreciate Geraldine Peters (University of Southern California) for providing us the characteristics of the primary star seen in her high-resolution spectroscopy. We wish to thank Jake Gersh and Christine Fennessey (see Fennessey et al. 2003), who as undergraduates at Georgia Tech obtained Wilson-Devinney solutions on the *UBV* photometry only. Our research made use of the SIMBAD database, operated at CDS, Strasbourg, France. The research at Tennessee State University has been supported in part by NSF grant AST-1039522 and the state of Tennessee through its Centers of Excellence program.

References

Allen, C. W. 2000, in Allen's Astrophysical Quantities, ed. A. N. Cox, (New York: Springer-Verlag), 388
Batten, A. H., Fletcher, J. M., & MacCarthy, D. G. 1989, PDAO, 17, 1
Bell, S. A., Kilkenny, D., & Malcolm, G. J. 1987, MNRAS, 226, 879
Brancewicz, H. K., & Dworak, T. Z. 1980, AcA, 30, 501
Budding, E. 1984, BICDS, 27, 91
Budding, E., Erdem, A., Çiçek, C., et al. 2004, A&A, 417, 263
Chiosi, C., & Maeder, A. 1986, ARA&A, 24, 329
Eaton, J. A., & Williamson, M. H. 2007, PASP, 119, 886
Fekel, F. C., & Griffin, R. F. 2011, Obs, 131, 283
Fekel, F. C., Tomkin, J., & Williamson, M. H. 2009, AJ, 137, 3900
Fennessey, C. M., Sowell, J. R., & Williamon, R. M. 2003, AAS, 203, 1250
Flower, P. J. 1996, ApJ, 469, 355
Hardie, R. H. 1962, in Astronomical Techniques, Vol. 2, Stars and Stellar Systems, ed. W. A. Hiltner, (Chicago, IL: Univ. Chicago Press), 178
Hilditch, R. W. 2005, Obs, 125, 72
Hilditch, R. W., & Bell, S. A. 1987, MNRAS, 229, 529
Hilditch, R. W., & Hill, G. 1975, MmRAS, 79, 101
Lazaro, C., Arevalo, M. J., & Almenara, J. M. 2009, NewA, 14, 528
Linnell, A. P., Etzel, P. B., Hubeny, I., & Olson, E. C. 1998, ApJ, 494, 773
Lucy, L. B. 1967, ZA, 65, 89
Nelson, C. A., & Eggleton, P. P. 2001, ApJ, 552, 664
Özdemir, S., Ak, H., Tanriver, M., et al. 2001, PASA, 18, 151
Pojmanski, G. 2002, AcA, 52, 397
Polidan, R. S., & Wade, R. A. 1991, BAAS, 23, 879
Scarfe, C. D. 2010, Obs, 130, 214
Shakhovskoy, N. M. 1955, PZ, 10, 309
Svechnikov, M. A., & Kuznetsova, E. F. 1990, (Sverdlovsk: Ural University Publication) Volumes 1, 2
Van Hamme, W. 1993, AJ, 106, 2096
Van Hamme, W., & Wilson, R. E. 1993, MNRAS, 262, 220
Van Hamme, W., & Wilson, R. E. 2007, ApJ, 661, 1129
Wilson, R. E. 1979, ApJ, 234, 1054
Wilson, R. E. 1990, ApJ, 356, 613
Wilson, R. E. 2012a, JASS, 29, 115
Wilson, R. E. 2012b, AJ, 144, 73
Wilson, R. E., & Devinney, E. J. 1971, ApJ, 166, 605
Wilson, R. E., & Van Hamme, W. 1986, AJ, 92, 1168
Wilson, R. E., Van Hamme, W., & Terrell, D. 2010, ApJ, 723, 1469
Wood, B. D., & Forbes, J. E. 1963, AJ, 68, 257
Zhao, E.-G., Qian, S.-B., Lajús, E. F., von Essen, C., & Zhu, L.-Y. 2010, RAA, 10, 438